International Journal of Nanoelectronics and Materials
IJNeaM
ISSN 198-5761 | E-ISSN 2232-1535

Effectiveness of Starch Nanocrystals on Mechanical and Shape Memory Behaviour of Smart Rubber

Yi Wei Tan[a], Ai Bao Chai[a,*], Kim Yeow Tshai[a], Jee Hou Ho[a], Shamsul Kamaruddin[b], and Andri Andriyana[c]

[a]*Department of Mechanical, Materials and Manufacturing Engineering, Faculty of Science and Engineering, University of Nottingham Malaysia, Jalan Broga, 43500 Semenyih, Selangor, Malaysia.*
[b]*Quality and Technical Services Division, Malaysian Rubber Board, Jalan Sungai Buloh, 47000 Sungai Buloh, Selangor, Malaysia.*
[c]*Centre of Advanced Materials, Department of Mechanical Engineering, Faculty of Engineering, University of Malaya, 50603 Kuala Lumpur, Malaysia.*
**Corresponding author. Tel.: +03-8924 8322; fax: +03-8924 8000; e-mail: AiBao.Chai@nottingham.edu.my*

ABSTRACT

Shape memory rubber (SMR) is a type of smart rubber that can undergo reversible changes when exposed to external stimuli such as temperature, solvent, pH, light, magnetic field and oxidation. Lightly crosslinked rubber demonstrated shape memory behaviour without any initial heat treatment. However, the strength of lightly crosslinked natural rubber latex (NRL) film cured by sulphur is relatively low. With the concept of sustainability in mind, the idea of fabricating green smart material for continuous development has motivated researchers to explore the realms of sustainable materials. This research aims to investigate the mechanical behaviour of starch nanocrystals (SNC) reinforced rubber composite films. To this end, the emphasis is laid on evaluating the effectiveness of SNC on shape memory effect (SME) of rubber nanocomposite films. In the current work, up to 8 wt% of SNC synthesized by acid hydrolysis was incorporated into NRL and the mixture was cast to form rubber nanocomposite films. SNC effectively increased the modulus and energy-storing potential of the rubber nanocomposite films. Moreover, the shape memory behaviour of the rubber nanocomposite films improved significantly with SNC content, leading to increased shape fixity (S_f) and full shape recovery (S_r).

Keywords: *Mechanical Behaviour, Rubber Nanocomposite Films, Shape Memory Effect, Shape Memory Rubber, Starch Nanocrystals*

1. INTRODUCTION

Smart materials are advanced materials with the ability to respond to external stimuli by altering their shape or behaviour enabling them to perform specific tasks in a controlled manner and distinguish themselves from the ordinary materials. One class of smart materials are shape memory polymers (SMPs) that can be programmed to a temporary shape before triggering the recovery process to return to their original shape by light [1] or temperature [2-3] makes them an intriguing prospect to become an essential matter of research within the field of material engineering. SMPs present many advantages such as low cost, ease of processability, high shape recoverability and biodegradability raised tremendous attention for various applications, particularly in medical devices, actuators, sensors and other smart devices [4–6]. These SMPs are usually crosslinked to a certain extent to retain their original permanent shape while possessing a glass transition or crystalline melting region responsible for impeding the recovery process during a shape memory cycle.

The most widely studied SMPs are segmental crosslinked polyurethane which SME deteriorates upon cyclic deformation due to creeping [7-8]. Thus, it opens opportunities for the development of novel multi-functional SMPs. Despite many efforts in developing SMPs, elastomer based SMPs especially rubber still lack in-depth research due to their low glass transition temperature (T_g) that proved to be an obstacle to initiate S_f at room temperature. In fact, natural rubber (NR) is an ideal candidate to be developed into SMR because of its unique molecular arrangement that allows reversible changes when stress is applied and removed. SME in rubber can be realized if the temporary deformed shape is fixed in the absence of stress and returns to its original shape upon initiating the recovery process. Previous works have reported two strategies to induce SME in NR (i) strain-induced crystallization (SIC) in lightly crosslinked NR [9] and (ii) blending of NR with fatty acids that increased the T_g of the material [10]. From our recent investigations, the strength of lightly crosslinked NRL is relatively low due to the minimum amount of crosslinking agent [11]. Therefore, the use of reinforcing filler such as silica, graphene oxide, carbon nanoclay and carbon nanotubes is common to improve the mechanical strength and elastic modulus of rubber films [12].

Considering sustainability, the substitution of conventional fillers with eco-friendly bio-fillers is gaining wide acceptance for various applications, specifically in the rubber industry. In this sector, fillers play an important role to improve product performance. Starch is a naturally occurring abundant biodegradable polysaccharide that is found in most plants. In the past decades, nanomaterial derived from renewable sources has been used as a reinforcing filler in polymers having the term “green” bio-

nanocomposite [13]. SNC obtained from acid hydrolysis of native starch has been incorporated into different polymer matrices for enhancement of mechanical properties, solvent absorption, thermal properties and barrier properties [14]. Indeed, SNC had proved to be an effective nanofiller for enhancement of mechanical properties due to the ability of SNC to form three-dimensional networks and excellent filler-matrix interactions [14-17]. Nevertheless, previous works of literature have suggested the negative effect of filler on shape memory behaviour of SMPs [18-19]. In spite of this, increasing environmental awareness and emerging interest in SMPs have motivated researchers to contribute an immense amount of effort to developing multi-functional SMPs. Still, considerably little to no study had been reported on analysing the mechanical behaviour and SME of rubber nanocomposite films. This work aims to reaffirm the legitimacy of SME in lightly crosslinked NRL films. To this end, the mechanical behaviour of SNC reinforced NRL films was investigated with an emphasis on evaluating the effectiveness of SNC in improving shape memory behaviour of rubber nanocomposite films. It can be regarded as the first step towards fabrication and evaluation of novel sustainable bio-SMR with improved mechanical properties.

2. MATERIALS AND METHODS

2.1. Materials

Commercial grade low ammonia concentrated NRL with 61.84% total solid content, 60.16% dry rubber content and 0.30% alkalinity was purchased from Getahindus (M) Sdn Bhd. The compounding chemicals in dispersion form such as sulphur, zinc dibutyldithiocarbamate (ZDBC) and zinc oxide (ZnO) were supplied by Aquaspersion (M) Sdn Bhd. Industrially available waxy maize starch was supplied by Imextco (M) Sdn Bhd. Moisture content of the starch was measured between 11-14% with EN ISO 1666 method. This product is suitable for laboratory experiments as it complies with the requirements of EU Directives and Regulations on foods and foods ingredients.

2.2. Materials Preparation

2.2.1 Synthesising and Characterisation of SNC

Aqueous suspension of SNC was obtained through the optimised acid hydrolysis technique [20]. 36.725g of waxy maize starch was mixed with 250 mL of 3.16M sulphuric acid at 40 °C under a stirring speed of 100 rpm for 5 days. After 5 days of mechanical stirring, the suspension was centrifuged and washed successively with distilled water for 12 minutes at 7800 rpm by Eppendorf Centrifuge 5430 to achieve neutrality. A neutral suspension (confirmed by pH meter) was achieved after 8 subsequent centrifuging and washing cycles. At this stage, the native waxy maize starch was believed to be broken down into nanocrystals observed visually from changes in the refractive index of the solution. Next, the aqueous suspension was sent for ultrasonic treatment at 50% amplitude for 10 minutes to disperse aggregates. A few drops of chloroform were then added into the SNC aqueous suspension to prevent the growth of bacteria before storing in a 4 °C refrigerator.

The morphology of the synthesized SNC was studied using a Field Emission Scanning Electron Microscope (FESEM), FEI QUANTA 400F. Aqueous suspension of SNC was mounted on an aluminium specimen holder before being inserted into the testing equipment. The sample was tested at 10kV with 3000 times magnification under vacuum conditions.

Particle size distribution of SNC was analysed using Malvern Panalytical Nano-Zetasizer. Aqueous suspension of SNC was placed on a quartz cuvette before running the analyzer at 25 °C for 60s. Water with a refractive index of 1.33 and viscosity of 0.89 mPa.s was used as a dispersant for the test.

2.2.2 Fabrication of Lightly Crosslinked NRL films

NRL was mixed with the chemical compounds shown in Table 1. Different loadings of sulphur were introduced to evaluate the effect of crosslink density on shape memory behaviour of the rubber films. Low content of sulphur is presented because the formed crystals upon deformation remain after releasing the stretching force and stabilising the rubber network in a highly elongated state for lightly crosslinked rubber films [12]. Firstly, the mixtures were continuously stirred using a magnetic stirrer at room temperature under a stirring speed of 200 rpm for 60 minutes to ensure uniform dispersion. The homogenous mixtures were then casted on petri dishes and glass moulds to form thin rubber films. Subsequently, the casted rubber films were heated to 50 °C and conditioned for 5 hours. Vulcanised rubber films were stored at room temperature for 7 days to allow complete drying. After 7 days, the dried rubber films were removed from petri dishes and glass moulds before cutting into rubber strips with dimensions 30mm x 10mm x 1mm and 150mm x 150mm x 0.3mm respectively.

Table 1 Formulation of lightly crosslinked NRL films

Samples	Sulphur (phr)	ZDBC (phr)	ZnO (phr)
NRL 0.0	0.00	0.00	0.00
NRL 0.2	0.20	0.40	0.25
NRL 0.3	0.30	0.50	0.25
NRL 0.4	0.40	0.60	0.25
NRL 2.0	2.00	1.00	0.25

2.2.3 Fabrication of SNC Reinforced Rubber Composite Films

From Figure 3(a) and (b), rubber film with 0.2 phr sulphur content exhibited the best overall shape memory behaviour thus all rubber nanocomposite films were crosslinked with this amount of sulphur. The corresponding loadings of ZDBC and ZnO were 0.40 and 0.25, respectively. Table 2 shows the amount of SNC incorporated into NRL. Firstly, SNC aqueous suspension

and compounded NRLs were stirred with a magnetic stirrer at 200rpm for 15 minutes to ensure uniform dispersion of the mixtures. Next, the mixtures were placed in an ultrasonic bath operating under degas mode with 35kHz frequency and 60% amplitude for 10 minutes to prevent the formation of irreversible bubbles during the drying process. Then, the well-dispersed mixtures were casted on petri dishes and glass moulds before evaporating in a ventilated oven at 70 °C for 3 hours and subsequently heated at 105 °C for 30 minutes. The dried rubber nanocomposite films were conditioned at room temperature for 7 days before cutting into rubber strips with 1mm and 0.3mm thicknesses.

Table 2 SNC content in rubber nanocomposite films

Samples	SNC (dry wt%)
NRL/SNC 0%	0.00
NRL/SNC 2%	2.00
NRL/SNC 4%	4.00
NRL/SNC 6%	6.00
NRL/SNC 8%	8.00

2.3. Characterization and Shape Memory Behavior of Smart Rubber

2.3.1 Dynamic Mechanical Analysis (DMA)

DMA was performed using Dynamic Mechanical Analyser 8000 PerkinElmer to relate the effect of SNC on storage modulus (E') and tan δ peaks of the reinforced rubber composite films. In each test, rubber nanocomposite film with dimensions (30 x 10 x 1mm) was loaded with static force of 0.5N, 2.0 force multiplier and 0.1mm strain under tensile mode. The operating frequency was 1Hz while the scanning temperature was programmed from -60 to 110 °C at 2°C/min. Purging of liquid nitrogen was done to achieve the required testing conditions. Rubbery storage tensile modulus at a temperature of 25° C (E'_{25}) was identified to evaluate the reinforcing effect of SNC at temperatures higher than T_g. This analysis revealed the evolution of E' and tan δ against temperature within the investigated range.

2.3.2 Evaluation of Shape Memory Behavior

A thermomechanical cycle was performed using a special elongation device operating under strain-controlled mode to investigate the SME of lightly crosslinked rubber films and rubber nanocomposite films. A rubber specimen with dimensions of 30mm x 10mm x 1mm was secured by two stainless steel clips that acted as clamps. Initially, each rubber specimen was marked with a 1cm gap that acted as initial strain (ε_i) before clamping on the special elongation device. Then, the rubber specimen was stretched at room temperature of 25 °C to 600% deformation and the elongated length was recorded as loading strain (ε_l). The ε_l is determined from tensile test that suggested the rubber films having elongation at break of more than 700%. Thus, 600% is used as ε_l to prevent the overstretching of the specimens. Subsequently, the rubber specimen was immediately quenched in 4 °C ice water for 120s to fix the temporary shape. The stretched sample was then unloaded from the clips and fixed strain (ε_f) was recorded. The recovery process was induced at 37 °C and the recovery strain was measured (ε_r). Accuracy of all the measured length was kept within ±0.5mm. S_f and S_r of the rubber specimen were then calculated from Equations 1 and 2 after one shape memory cycle.

$$S_f\,(\%) = (\varepsilon_f / \varepsilon_l) \times 100 \quad (1)$$

$$S_r\,(\%) = (\varepsilon_l - \varepsilon_r) / (\varepsilon_l - \varepsilon_i) \times 100 \quad (2)$$

3. RESULTS AND DISCUSSION

3.1. Morphology and Particle Size Distribution of SNC

The morphology and particle size distribution of SNC as determined from FESEM and particle size analysis were presented in Figure 1. It can be seen from Figure 1(a) that SNC possessed a spherical shape, and no impurities nor aggregates were found in the micrograph. This scenario suggested that SNC was well dispersed in the suspension and the synthesised method was deemed to not create any impurities. However, some small parts of the SNC appeared to be in irregular spherical morphology with rough surface observed through the micrograph. It is attributed to the adhesion between starch granules and surface fracture that occurred during mechanical stirring and ultrasonic treatment process [21]. The size of SNC in nanoscale was proved by Figure 1(b). It is clearly shown that most of the SNCs were distributed in the size of approximately 600nm. The small part of SNC that was measured in the microscale is due to incomplete hydrolysis of native starch. It is because this microscale SNC measured to be 6μm showed equivalent size to native starch as revealed in Figure 1(c). This event can be optimised by filtering the SNC suspension before being incorporated into any matrices. Nonetheless, the findings from FESEM and Zetasizer analysis suggested that the synthesising method is effective as SNC dispersed homogenously in the aqueous suspension and the size was successfully reduced to the nanoscale.

3.2. Mechanical Behavior of SNC Reinforced Rubber Composite Films

Figures 2(a) and (b) show the plots of Log E' and tan δ against the temperature of the NRL nanocomposite films with varying SNC content. As revealed in Figure 2(a), the unfilled rubber matrix exhibited a typical high molecular weight thermoplastic behaviour. Moreover, from Figure 2(c), lightly crosslinked NRL films showed an analogous log E' trend to the unfilled matrix with decreasing E' against temperature until the glass-rubber transition zone.

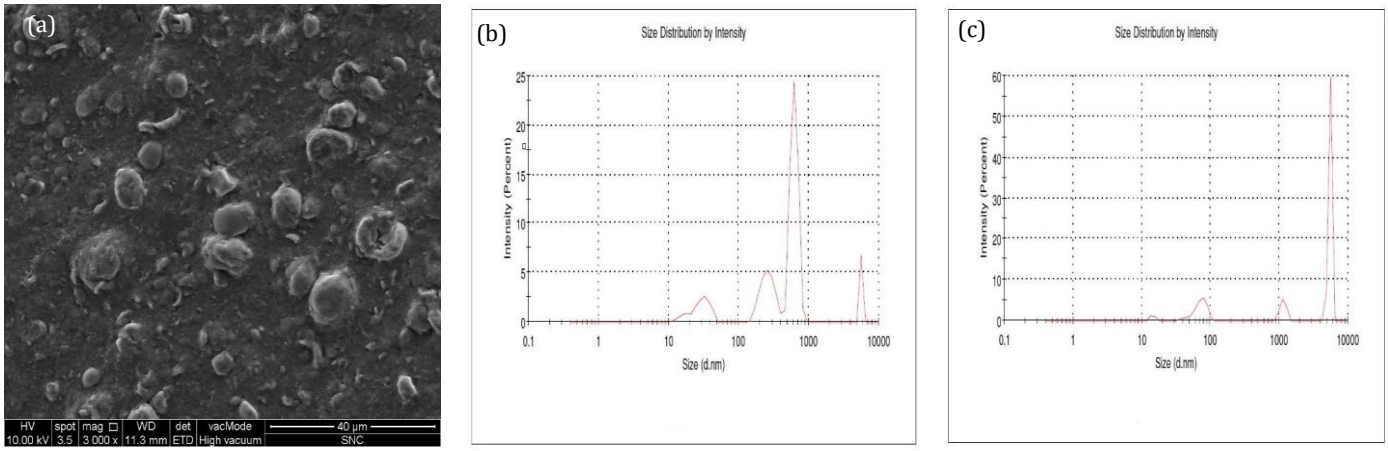

Figure 1. (a) FESEM micrograph of SNC and particle size and size distribution of (b) SNC (c) native starch.

Since NRL 0.2 and NRL/SNC 0% shared the same formulation, the trend of Log E' against temperature is very much alike between each other when comparing Figure 2(a) and (c). Indeed, rubber nanocomposite films showed a similar pattern to the unfilled matrix indicating the incorporation of SNC maintains the elastomeric properties along with viscoelastic behaviour within the material. The rubber nanocomposite films behave like a glassy material where they are rigid and brittle at a temperature below T_g with decreasing storage modulus against temperature but remain in the range of 1-3GPa. A sharp decrease of E' accounting to approximately 2-3 decades corresponding to the primary relaxation process related to glass-rubber transition which resulted in a damping scenario reflected in Figure 2(b). This sharp decrease of E' occurred at a temperature of -60 °C for NRL nanocomposite films. In fact, an obvious glass-rubber transition zone corresponding to the horizontal glassy region of the materials is not shown in Figure 2(a) and (c) due to the certainty surrounding Tg of NRL films being -65 °C [22]. The modulus then reached a broad rubbery plateau region that remained above 1MPa suggesting the flexibility, elasticity and capability of returning to its original shape for a wide range of temperatures. Indeed, the E' of SNC-filled rubber composite films are higher than the unfilled matrix at the rubbery region. This advocated that SNC possessed a significant reinforcing effect at temperatures higher than T_g. As shown in Table 3, the E'_{25} of rubber nanocomposites films containing 2%, 4%, 6% and 8% SNC are 1.64, 2.48, 3.25 and 4.45 times higher than the unfilled rubber matrix. This reinforcing effect is due to the formation of a robust network of SNC interconnected through strong hydrogen bonds and excellent filler-rubber interactions [23-24].

The evolution of tan δ against temperature displayed a peak located at T_g of the rubber nanocomposite films as shown in Figure 2(b). This relaxation process known as α-relaxation is associated with the anelastic behaviour observed during the glass-rubber transition of the material. SNC-filled rubber composite films have comparable T_g to unfilled rubber matrix which is at approximately -50 °C presented through the peak of temperature (T_α) displayed in Table 3. This finding is aligned with the result identified from other literature where the addition of SNC from different botanical origins on NR resulted in similar T_g [25]. Thus, it can be interpreted that the incorporation of SNC within the dosage of 2-8% will not directly affect the chain mobility that governs the T_g of a material. In the case of lightly crosslinked natural rubber, increasing sulphur loading resulted in a slight shift to the right of tan δ curves as shown in Figure 2(d). This is because higher crosslink density restricted the movement of rubbery chains that in turn increased T_g of the material. Moreover, the magnitude of tan δ peaks (I_α) were listed in Table 3. These values provide insight regarding the energy dissipation ability of the NRL nanocomposite films as the viscoelastic behaviour of rubber enables it to store part of the energy applied upon deformation and disperse the other part through viscous dissipation. It was found that SNC-reinforced NRL composite films possessed lower I_α than the unfilled rubber matrix. This is due to the reduced energy loss attributed to the decrease in molecular motions of the polymer chain which is the result of good intermolecular interactions between filler and matrix [26]. Therefore, rubber nanocomposite films act more elastic and have greater potential to store energy rather than dissipate it. This characteristic can be explored through the shape memory behaviour more particularly the ability to improve S_f within the rubber nanocomposite films.

Table 3 E'_{25}, T_α and I_α of NRL nanocomposite films

Samples	E'_{25} (MPA)	T_α (°C)	I_α
NRL/SNC 0%	0.73	-46.45	2.75
NRL/SNC 2%	1.20	-50.42	2.45
NRL/SNC 4%	1.81	-49.10	2.06
NRL/SNC 6%	2.37	-49.76	2.41
NRL/SNC 8%	3.25	-48.78	2.08

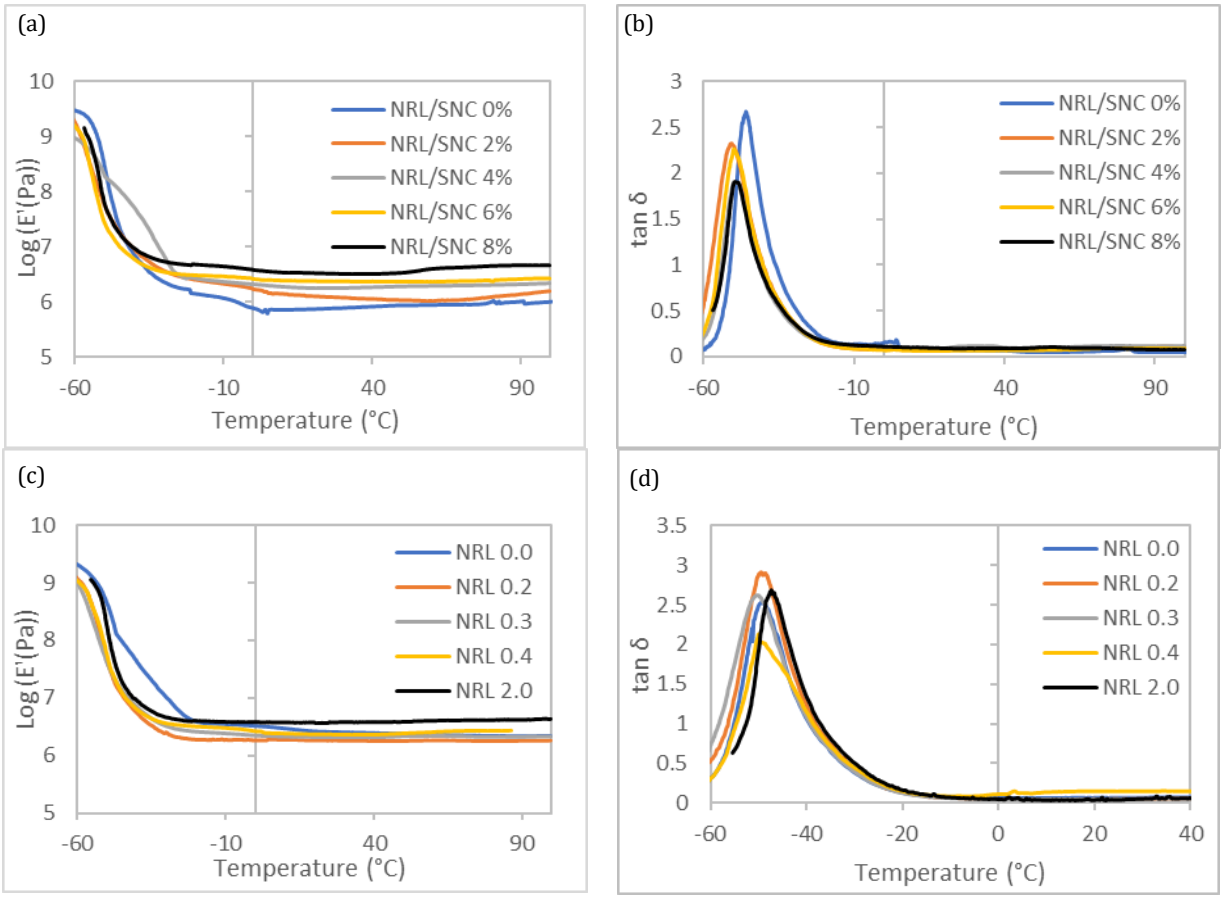

Figure 2. Plot of Log E' against temperature for (a) NRL nanocomposite films (c) lightly crosslinked NRL films and tan δ against temperature for (b) NRL nanocomposite films (d) lightly crosslinked NRL films.

3.3. Shape Memory Behavior of Smart Rubbers

Figure 3(a) and (b) show the SME of lightly crosslinked NRL films. As shown in Figure 3(a), crosslink density plays an important role in S_f of the rubber films. It was suggested that the crystallinity index decreased almost linearly with crosslink density due to the interruption of increasing chemical crosslinks [27]. Therefore, highly crosslinked NRL 2.0 failed to demonstrate any S_f as the rubber film restored its original shape immediately after releasing the stretching force. Accounting to the same reason, S_f ranking of the investigated lightly crosslinked rubber films is as follows: NRL 0.2, NRL 0.3, NRL 0.4. Interestingly, uncrosslinked rubber films referring to NRL 0.0 showed 50% of S_f. This is due to the existence of end-linked networks attributed from functional groups located at both ends of the rubber chains form linkages with natural impurities aided in the occurrence of SIC [28]. On the other hand, the lack of crosslinking in NRL 0.0 caused permanent plastic deformation that prevented full S_r of the rubber films as shown in Figure 3(b). Overall, NRL 0.2 exhibited the best SME achieving 75% Sf and 100% S_r. This finding suggested that within the investigated context, 0.2phr sulphur is the ideal content for the development of SMR that is capable of keeping the rubber films constraint at high elongation with no plastic deformation upon the activation of S_r.

Rubbers hold significant promise for being categorised as smart material owing to its exceptional molecular structure and distinctive physical properties. In the case of NRL films, the rubber matrix is an amorphous polymer at room temperature that crystallises under strain and promptly reverts to its initial shape upon the release of stretching force while the crystals disappear during this process. Furthermore, T_g of NRL that is well below room temperature obstructs its necessary properties to exhibit SME. However, crosslinking of NRL at the borderline between thermoplastic and elastomer enables the development of stable SIC at room temperature. This characteristic can fix the temporary network at a highly elongated state and return to its original shape at a temperature of around 37 °C. The heterogeneity of crosslinked network points and short chain structure of the network regions lead to preferential growth of crystals under tensile deformation [29]. These elements provide the necessity for NRL to be the first SMP that can be programmed without initial heat treatment.

It was realised that NRL 0.2 achieved the best overall SME among the other lightly crosslinked NRL films. Therefore, every NRL nanocomposite film with varying SNC dosage was crosslinked with 0.2 phr of sulphur. Figure 3(c) and (d) reveal the SME of NRL nanocomposite films programmed at room temperature. It was shown in Figure 3(c) that S_f of the rubber nanocomposite films increased with SNC content. This is primarily because of the increased crystallinity of the material that resulted in

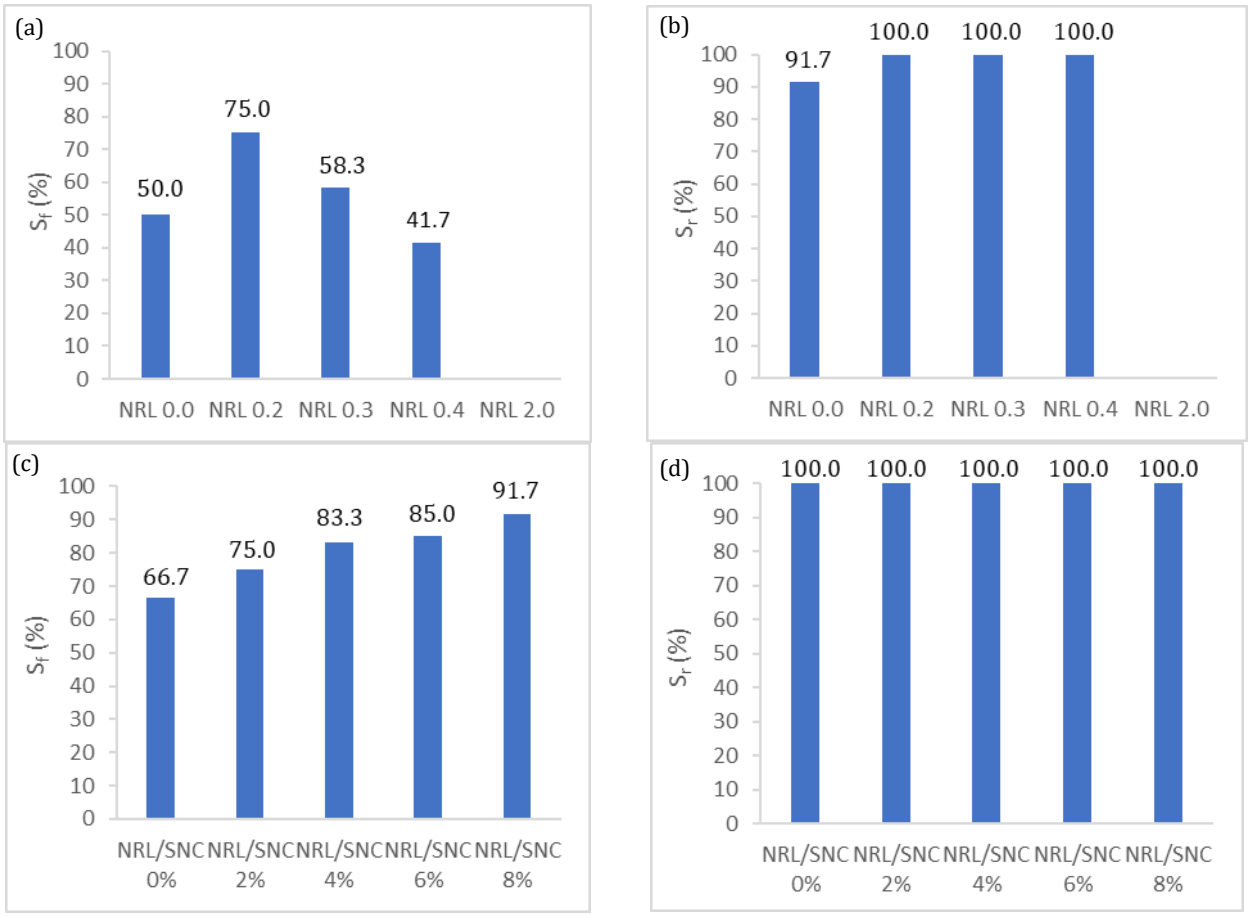

Figure 3 SME of (a) & (b) lightly crosslinked NRL films, and (c) & (d) NRL nanocomposite films

improved SIC of the NRL nanocomposite films. Two clear mechanisms of crystallisation were noted for rubber nanocomposite films which are in contrast to the single step of crystallisation observed in unfilled rubber films [30-31]. The first phase is associated with the alignment of nanofillers during deformation whereas the second phase was ascribed to the typical SIC of rubber matrix. Thus, strong orientation in the direction of stretching provides SNC the fundamental condition to act as effective nucleation sites for formation of crystallites within the rubber. This circumstance developed a more orderly arranged macroscopic rubber structure which enhanced the phenomenon relating to SIC therefore resulted in increased S_f of SNC-reinforced composite films. Such finding has also been reported on carbon nanodots filled NR composites [32]. The upper limit of S_f achieved by NRL nanocomposite films is 91.7% corresponding to NRL/SNC 8%. As a result, the incorporation of 8% SNC to NRL improved the S_f of the rubber nanocomposite films by 37% compared to the unfilled matrix. Moreover, as revealed in Figure 3(d), no negative effect was observed on S_r of the investigated rubber films. In fact, all filled and unfilled rubber films exhibited 100% S_r over a single shape memory cycle indicating the absence of plastic deformation. As a comparison to other fillers, carbon nanotubes filled NR/paraffin wax blend exhibited 93% S_f and 82.7% S_r resembling the presence of permanent deformation [33].

Therefore, it can be interpreted that the incorporation of SNC increased the shape fixing capability while maintaining the elasticity of the rubber nanocomposite films. This demonstrated the effectiveness of SNC in enhancing the shape memory behaviour of smart rubber.

4.0 CONCLUSION

In this work, the mechanical and shape memory behaviour of smart rubbers have been systematically explored. Additionally, the effectiveness of the SNC synthesising method is evident from the homogenous dispersion of SNC aqueous suspension, as demonstrated by FESEM. The successful breakdown of native starch into nanoscale particles is also confirmed. There are no significant challenges faced during the incorporation of SNC into rubber latex apart from the considerably long synthesising time for SNC. It was found that SNC is an effective reinforcing filler for NRL as E'_{25} of rubber nanocomposite films constantly surpasses that of the unfilled rubber matrix. Moreover, the incorporation of SNC into NRL has a negligible effect on T_g while increasing the energy-storing potential of the material. Lightly crosslinked NRL films exhibited shape memory behaviour with NRL 0.2 demonstrating the most promising overall SME performance, featuring 75% S_f and 100% S_r. The roles of SIC and the degree of crosslink density were found to be significant in developing SMEs within lightly crosslinked rubber films. Moreover, NRL nanocomposite films have consistently displayed higher SME compared to the

unfilled matrix attributed to the increase in SIC and crystallinity of the materials. Within the investigated range, the upper limit of SME was demonstrated by NRL/SNC 8% achieving 91.7% S_f and 100% S_r. Thus, it can be inferred that SNC effectively enhances the shape memory behaviour of rubber films. Durability test for the long-term performance evaluation of the smart rubber will be taken into account as future work. Furthermore, more characterisation works such as X-ray diffraction (XRD) will be performed to further ascertain the presence of SNC in the SMR.

ACKNOWLEDGMENTS

This research is financially supported by the Ministry of Higher Education, Malaysia under the Fundamental Research Grant Scheme (Grant number: FRGS/1/2021/TK0/UNIM/02/4).

REFERENCES

[1] A. Lendlein, H. Jiang, O. Jünger, and R. Langer, "Light-induced shape-memory polymers," Nature, vol. 434, no. 7035, pp. 879–882, Apr. 2005, doi: 10.1038/nature03496.

[2] H. Luo et al., "Temperature sensing of conductive shape memory polymer composites," Mater. Lett., vol. 140, pp. 71–74, Feb. 2015, doi: 10.1016/j.matlet.2014.11.010.

[3] S. K. Dogan, S. Boyacioglu, M. Kodal, O. Gokce, and G. Ozkoc, "Thermally induced shape memory behavior, enzymatic degradation and biocompatibility of PLA/TPU blends: 'Effects of compatibilization,'" J. Mech. Behav. Biomed. Mater., vol. 71, no. March, pp. 349–361, 2017, doi: 10.1016/j.jmbbm.2017.04.001.

[4] A. Lendlein and R. Langer, "Biodegradable, elastic shape-memory polymers for potential biomedical applications," Science (80-.)., vol. 296, no. 5573, pp. 1673–1676, 2002, doi: 10.1126/science.1066102.

[5] C. Liu, H. Qin, and P. T. Mather, "Review of progress in shape-memory polymers," J. Mater. Chem., vol. 17, no. 16, pp. 1543–1558, 2007, doi: 10.1039/b615954k.

[6] J. Leng, H. Lu, Y. Liu, W. M. Huang, and S. Du, "Shape-memory polymers - A class of novel smart materials," MRS Bull., vol. 34, no. 11, pp. 848–855, 2009, doi: 10.1557/mrs2009.235.

[7] J. R. Lin and L. W. Chen, "Study on shape-memory behavior of polyether-based polyurethanes. I. Influence of the hard-segment content," J. Appl. Polym. Sci., vol. 69, no. 8, pp. 1563–1574, Aug. 1998, doi: 10.1002/(SICI)1097-4628(19980822)69:8<1563::AID-APP11>3.0.CO;2-W.

[8] B. K. Kim et al., "Polyurethane ionomers having shape memory effects," Polymer (Guildf)., vol. 39, no. 13, pp. 2803–2808, Jun. 1998, doi: 10.1016/S0032-3861(97)00616-2.

[9] F. Katzenberg and J. C. Tiller, "Shape memory natural rubber," J. Polym. Sci. Part B Polym. Phys., vol. 54, no. 14, pp. 1381–1388, 2016, doi: 10.1002/polb.24040.

[10] N. R. Brostowitz, R. A. Weiss, and K. A. Cavicchi, "Facile fabrication of a shape memory polymer by swelling cross-linked natural rubber with stearic acid," ACS Macro Lett., vol. 3, no. 4, pp. 374–377, 2014, doi: 10.1021/mz500131r.

[11] Y. Y. Kow, A. B. Chai, and J. H. Ho, "Relationships between swelling temperature and shape memory properties of palmitic acid-based shape memory natural rubber," J. Rubber Res., vol. 23, no. 1, pp. 13–22, 2020, doi: 10.1007/s42464-019-00031-w.

[12] A. Reghunadhan, K. Jibin, A. Kaliyathan, P. Velayudhan, M. Strankowski, and S. Thomas, "Shape Memory Materials from Rubbers," Materials (Basel)., vol. 14, no. 23, pp. 1–19, 2021, doi: 10.3390/ma14237216.

[13] M. Darder, P. Aranda, and E. Ruiz-Hitzky, "Bionanocomposites: A New Concept of Ecological, Bioinspired, and Functional Hybrid Materials," Adv. Mater., vol. 19, no. 10, pp. 1309–1319, May 2007, doi: 10.1002/adma.200602328.

[14] N. Lin, J. Huang, P. R. Chang, D. P. Anderson, and J. Yu, "Preparation, modification, and application of starch nanocrystals in nanomaterials: A review," J. Nanomater., vol. 2011, 2011, doi: 10.1155/2011/573687.

[15] K. R. Rajisha, H. J. Maria, L. A. Pothan, Z. Ahmad, and S. Thomas, "Preparation and characterization of potato starch nanocrystal reinforced natural rubber nanocomposites," Int. J. Biol. Macromol., vol. 67, pp. 147–153, 2014, doi: 10.1016/j.ijbiomac.2014.03.013.

[16] K. Anand, S. Varghese, T. Kurian, and S. Bose, "Effect of starch nanocrystals on natural rubber latex vulcanizate properties," Prog. Rubber, Plast. Recycl. Technol., vol. 34, no. 2, pp. 75–87, 2018, doi: 10.1177/147776061803400201.

[17] Y. J. S. Gao, S. Zhao, S. Q. Liao, L. Fang, Z. F. Wang, and L. F. Li, "Reinforcement of natural rubber latex film by starch nanocrystal," Appl. Mech. Mater., vol. 543–547, pp. 3886–3891, 2014, doi: 10.4028/www.scientific.net/AMM.543-547.3886.

[18] K. Gall, M. Dull, Y. Liu, D. Finch, M. Lake, and N. Munshi, "Shape memory polymer nanocomposites," Acta Mater., vol. 50, no. 20, pp. 5115–5126, Dec. 2002, doi: 10.1016/S1359-6454(02)00368-3.

[19] T. Ohki, Q.-Q. Ni, N. Ohsako, and M. Iwamoto, "Mechanical and shape memory behavior of composites with shape memory polymer," Compos. Part A Appl. Sci. Manuf., vol. 35, no. 9, pp. 1065–1073, Sep. 2004, doi: 10.1016/j.compositesa.2004.03.001.

[20] H. Angellier, L. Choisnard, S. Molina-Boisseau, P. Ozil, and A. Dufresne, "Optimization of the preparation of aqueous suspensions of waxy maize starch nanocrystals using a response surface methodology," Biomacromolecules, vol. 5, no. 4, pp. 1545–1551, 2004, doi: 10.1021/bm049914u.

[21] R. G. Utrilla-Coello et al., "Acid hydrolysis of native corn starch: Morphology, crystallinity, rheological and thermal properties," Carbohydr. Polym., vol. 103, no. 1, pp. 596–602, 2014, doi: 10.1016/j.carbpol.2014.01.046.

[22] C. C. Ho and M. C. Khew, "Low Glass Transition Temperature (T g) Rubber Latex Film Formation Studied by Atomic Force Microscopy," Langmuir, vol. 16, no. 6, pp. 2436–2449, Mar. 2000, doi: 10.1021/la990192f.

[23] A. Dufresne, "Natural Rubber Green Nanocomposites," in Rubber Nanocomposites: Preparation, Properties and Applications, 1st ed., S. Thomas and R. Stephen, Eds. Wiley, 2010, pp. 113–145.

[24] P. Mélé, H. Angellier-Coussy, S. Molina-Boisseau, and A. Dufresne, "Reinforcing Mechanisms of Starch Nanocrystals in a Nonvulcanized Natural Rubber Matrix," Biomacromolecules, vol. 12, no. 5, pp. 1487–1493, May 2011, doi: 10.1021/bm101443a.

[25] D. S. LeCorre, J. Bras, and A. Dufresne, "Influence of the Botanic Origin of Starch Nanocrystals on the Morphological and Mechanical Properties of Natural Rubber Nanocomposites," Macromol. Mater. Eng., vol. 297, no. 10, pp. 969–978, Oct. 2012, doi: 10.1002/mame.201100317.

[26] N. I. N. Haris et al., "Dynamic mechanical properties of natural fiber reinforced hybrid polymer composites: a review," J. Mater. Res. Technol., vol. 19, pp. 167–182, Jul. 2022, doi: 10.1016/j.jmrt.2022.04.155.

[27] G. Femina et al., "X-ray diffraction study of strain-induced crystallization of hydrogenated nitrile-butadiene rubbers: Effect of crosslink density," Polymer (Guildf)., vol. 271, no. January, p. 125782, 2023, doi: 10.1016/j.polymer.2023.125782.

[28] S. Toki, B. S. Hsiao, S. Amnuaypornsri, and J. Sakdapipanich, "New insights into the relationship between network structure and strain-induced crystallization in un-vulcanized and vulcanized natural rubber by synchrotron X-ray diffraction," Polymer (Guildf)., vol. 50, no. 9, pp. 2142–2148, 2009, doi: 10.1016/j.polymer.2009.03.001.

[29] M. Tosaka et al., "Orientation and Crystallization of Natural Rubber Network As Revealed by WAXD Using Synchrotron Radiation," Macromolecules, vol. 37, no. 9, pp. 3299–3309, May 2004, doi: 10.1021/ma0355608.

[30] J. Carretero-Gonzalez, R. Verdejo, S. Toki, B. S. Hsiao, E. P. Giannelis, and M. A. López-Manchado, "Real-time crystallization of organoclay nanoparticle filled natural rubber under stretching," Macromolecules, vol. 41, no. 7, pp. 2295–2298, 2008, doi: 10.1021/ma7028506.

[31] G. Weng, G. Huang, L. Qu, Y. Nie, and J. Wu, "Large-scale orientation in a vulcanized stretched natural rubber network: Proved by in situ synchrotron x-ray diffraction characterization," J. Phys. Chem. B, vol. 114, no. 21, pp. 7179–7188, 2010, doi: 10.1021/jp100920g.

[32] B. Liu, S. Wang, J. Liu, Z. Tang, and B. Guo, "Promoted strain-induced crystallization of cis-1, 4-polyisoprene with functional carbon nanodots," Adv. Ind. Eng. Polym. Res., vol. 2, no. 1, pp. 25–31, 2019, doi: 10.1016/j.aiepr.2019.01.002.

[33] S. M. Lai and G. L. Guo, "Two-way shape memory effects of sulfur vulcanized natural rubber (NR) and NR/paraffin wax (PW)/carbon nanotube (CNT) nanocomposites," Polym. Test., vol. 77, no. February, p. 105892, 2019, doi: 10.1016/j.polymertesting.2019.05.008.